MERCURY'S LITHOSPHERIC MAGNETIC FIELD. Catherine L. Johnson[1,2], Roger J. Phillips[3,4], Lydia C. Philpott[1], Brian J. Anderson[5], Paul K. Byrne[6], Brett W. Denevi[5], Kevin Fan[1], Joshua M. Feinberg[7], Steven A. Hauck, II[8], James W. Head III[9], Haje Korth[5], Erwan Mazarico[10], Gregory A. Neumann[10], Michael E. Purucker[10], Becky M. Strauss[7], and Sean C. Solomon[11,12], [1]Dept.of Earth, Ocean and Atmospheric Sciences, University of British Columbia, Vancouver, BC, V6T 1Z4, Canada, cjohnson@eos.ubc.ca. [2]Planetary Science Institute, Tucson, AZ 85719, USA, cjohnson@psi.edu. [3]Planetary Science Directorate, Southwest Research Institute, Boulder, CO 80302, USA. [4]Dept. of Earth and Planetary Sciences, Washington University, St Louis, MO 63130, USA. [5]The Johns Hopkins University Applied Physics Laboratory, Laurel, MD 20723, USA. [6]Dept. of Marine, Earth, and Atmospheric Sciences, North Carolina State University, Raleigh, NC, 27695, USA. [7]Institute for Rock Magnetism, Department of Earth Sciences, University of Minnesota, Minneapolis, MN 55455, USA. [8]Department of Earth, Environmental, and Planetary Sciences, Case Western Reserve University, Cleveland, OH 44106, USA. [9]Department of Earth, Environmental and Planetary Sciences, Brown University, Providence, RI 02912, USA. [10]NASA Goddard Space Flight Center, Greenbelt, MD 20771, USA. [11]Lamont-Doherty Earth Observatory, Columbia University, Palisades, NY 10964, USA. [12]Department of Terrestrial Magnetism, Carnegie Institution of Washington, Washington, DC 20015, USA.

Overview. Observations made by the MESSENGER spacecraft in orbit around Mercury at altitudes less than ~100 km have revealed magnetic fields of lithospheric origin. Initial identifications of such fields [1] have been confirmed by the spatially extensive low-altitude observations that cover much of the northern hemisphere. Lithospheric fields are weak, typically a few nT to about 30 nT at spacecraft altitudes, and the shortest wavelengths observed are a few tens of km, even at spacecraft altitudes less than 10 km above the surface of the planet. We investigate magnetization distributions compatible with the observations and calculate the corresponding altitude-normalized maps of the magnetic field. The strongest magnetizations and magnetic fields are spatially associated with the Caloris and circum-Caloris region. Elsewhere, magnetization and magnetic field amplitudes are weaker and exhibit shorter coherence length scales, including over the northern volcanic plains. Magnetic field signatures are often, but not always, associated with impact basin interiors and/or ejecta materials. We discuss the implications of these results for the spatial and depth distributions and the origin(s) of magnetization in Mercury's lithosphere.

Observations. During the low-altitude campaign at the end of MESSENGER's orbital mission, magnetic field measurements were acquired at altitudes less than 100 km at all body-fixed longitudes from ~35°N to ~80°N (Figure 1). Lithospheric signals were identified by first subtracting contributions from the major magnetospheric fields [2], followed by high-pass-filtering, using the approach described earlier [1].

The resulting high-pass-filtered field shows signals over many regions (Figure 2), including repeat coverage of the signals initially identified over Suisei Planitia and the region south of Carnegie Rupes [1]. The strongest fields occur in the region 120°E to 210°E, a region that includes both smooth and heavily cratered terrain to the north and northwest of the Caloris impact basin. Weaker signals characterize heavily cratered terrain in other regions and the northern volcanic plains.

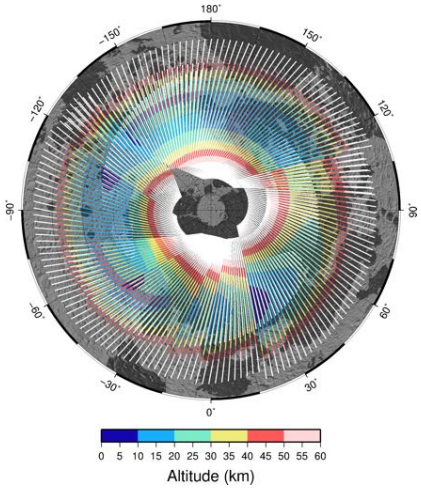

Figure 1. Spacecraft altitudes along orbit segments for which the spacecraft altitude was less than 100 km, and for which local times were between 1600 and 0800. Additional coverage between 0800 and 1600 was obtained in the longitude band ~310° E to 230° E. Background image shows smooth plains (dark gray) and intercrater plains (light gray) [3]. Lambert azimuthal equal area projection from 30° to 90° N.

We examined profiles from orbits with periapsis altitudes less than ~10 km and found them to exhibit a variety of signals. Some orbits show no substantial signal even at these very low altitudes, e.g., over the heavily cratered Victoria Rupes region. Other orbits show signals clearly associated with geological features, e.g., Strindberg crater (53°N, 194°E, D = 187 km) shows clear signals associated with the crater rim and the peak ring within the basin interior.

Modeling Approach. We conducted inversions for magnetization distributions using an equivalent source dipole technique [4] with regularization [5]. Our inversions used a single equivalent source layer and a dipole

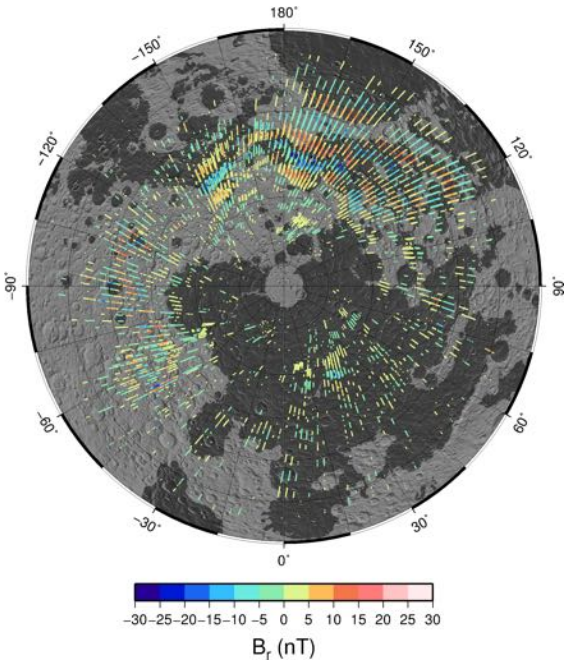

Figure 2. Map of high-pass-filtered radial field (B_r). Signals are shown only if the magnitude of B_r is at least 1 nT and if the signal-to-noise ratio is at least 4.

spacing of ~20 km. The magnetization model corresponding to the corner of the L-curve [see, e.g., 5] was used to calculate an altitude-normalized map of B_r, the radial component of the magnetic field (Figure 3). We constrained the magnetization direction to be that acquired in an axial dipole field because of the non-uniqueness inherent in such inversions. Data from anomalous orbits (e.g., during coronal mass ejections) were excluded. We verified consistency of our solutions for inversions of: B_r only versus the full vector field; data from the nightside versus all local times; a variety of constraints on magnetization direction; different solution methods (e.g., conjugate gradient, singular value decomposition); and dipole grid design. For the model shown in Figure 3, the reduction in variance was over 95% with a final root-mean-square misfit to the data of just under 0.7 nT.

Discussion. The strongest magnetizations (0.1–0.4 Am^{-1} for a 10-km-thick layer) and magnetic fields and the largest coherence length scales are spatially associated with the Caloris and circum-Caloris region, but the relationship of the magnetization to the origin and evolution of Caloris is not yet established. Elsewhere, magnetization and magnetic field amplitudes are weaker and exhibit shorter coherence length scales. The large coherence length scales and absence of very short-wavelength features in the lithospheric fields suggests that shallow crustal sources, if present, are very weak.

The relationship of lithospheric fields to craters is complex and not a simple function of crater diameter: stronger fields and magnetization contrasts are associated with some, but not all crater interiors and/or surrounding ejecta. Contributing factors might include pre-impact magnetization and the thermal history of a specified region, as well as local crustal thickness.

Induced and viscous remanent contributions to the magnetization are possible but cannot entirely account for the observed lithospheric fields. For example, if the observed fields result from magnetization entirely induced in the present field then layer thicknesses in excess of 100 km are required. This implies at least some contribution from a stable thermal remanence [2]. No obvious modulation of the magnetization signals by the thermal insolation signature is seen, suggesting that the magnetized layers lie at depths substantially shallower than the minimum depth (for orbital eccentricities experienced since remanence acquisition [1]) to the relevant Curie isotherm.

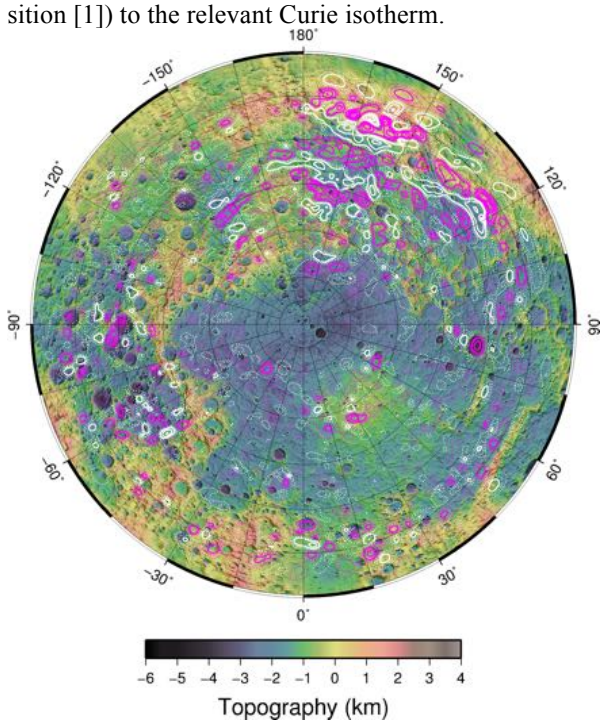

Figure 3. Map of B_r at 20 km altitude predicted by the magnetization model described in the text. White (magenta) contours denote positive (negative) B_r values. Contour interval is 6 nT (thick lines); thin dotted lines denote ±2 nT and ±4 nT contours. Projection as in Figure 1, with grid lines every 10° of latitude and 15° of longitude. Underlying image is topography derived from the Mercury Laser Altimeter.

References. [1] C. L. Johnson et al. (2015) *Science*, 348, 892. [2] H. Korth et al. (2015) *JGR Space Physics*, 120, 4503. [3] B. W. Denevi et al. (2013) *JGR Planets*, *118*, 891. [4] B. Langlais et al. (2004) *JGR*, 109, E02008. [5] R. C. Aster et al. (2013) *Parameter Estimation and Inverse Problems*, 2nd ed., Academic Press.